Polarization distortion effects in polarimetric two-photon microscopy

Peter Schön,[1] Fabiana Munhoz,[1] Alicja Gasecka,[1,2] , Sophie Brustlein,[1] and Sophie Brasselet,[1,*]

[1]*Institut FRESNEL, MOSAIC, Domaine Universitaire St Jérôme, 13397 Marseille, France*
[2]*Institut D'Alembert, Laboratoire de Photonique Quantique et Moléculaire, ENS Cachan, 61 av. du président Wilson, 94235 Cachan, France*
[*]*Corresponding author: sophie.brasselet@fresnel.fr*

Abstract: We present a global analysis of experimental factors affecting polarization responses in two-photon inverted microscopy. The role of reflection optics and high numerical aperture focusing is investigated in two-photon fluorescence, which can be extended to other nonlinear processes. We show that both effects strongly distort polarization responses and can lead to misleading extraction of molecular order information from polarimetric measurements. We describe a model accounting for these effects and develop a calibration technique for the determination of polarization parameters in the sample plane using two-photon fluorescence polarimetry in liquids.

OCIS codes: (180.4315) Nonlinear microscopy; (120.5410) Polarimetry.

References and links

1. J. A. Dix and A. S. Verkman, "Mapping of fluorescence anisotropy in living cells by ratio imaging," Biophys. J. **57**, 231-240 (1990).
2. T. H. Foster, B. D. Pearson, S. Mitra, and C. E. Bigelow, "Fluorescence anisotropy imaging reveals localization of meso-tetrahydroxyphenyl chlorin in the nuclear envelope," Photochem. Photobiol. **81**, 1544-1547 (2005).
3. J. Borejdo and S. Burlacu, "Measuring Orientation of Actin Filaments within a Cell: orientation of Actin in Intestinal Microvilli," Biophys. J. **65** 300-309 (1993).
4. R. K. P. Benninger, Björn önfelt, M. A. A. Neil, D. M. Davis, and P. M. W. French, "Fluorescence Imaging of Two-Photon Linear Dichroism: Cholesterol Depletion Disrupts Molecular Orientation in Cell Membranes," Biophys. J. **88** 609–622 (2005).
5. R. E. Dale, S. C. Hopkins,U. A. an der Heide, T. Marszałek, M. Irving, and Y. E. Goldman, "Model-Independent Analysis of the Orientation of Fluorescent Probes with Restricted Mobility in Muscle Fibers," Biophys. J. **78** 1606–1618 (1999).
6. A. M. Vrabioiu and T. J. Mitchison, "Structural insights into yeast septin organization from polarized fluorescence microscopy," Nature **443**, 466-468 (2006).
7. T. E. Schaus, E. W. Taylor, and G. G. Borisy, "Self-organization of actin filament orientation in the dendritic-nucleation/array-treadmilling model," Proc. Nat. Acad. Sc. **104**, 7086–7091 (2007).
8. D. A. Dombeck, K. A. Kasischke, H. D. Vishwasrao, M. Ingelsson, B. T. Hyman, and W. W. Webb, "Uniform polarity microtubule assemblies imaged in native brain tissue by second harmonic generation microscopy," Proc. Nat. Acad. Sc. **100**, 7081-7086 (2003).
9. D. Débarre, W. Supatto, A. M. Pena, A. Fabre, T. Tordjmann, L. Combettes, M. C. Schanne-Klein, and E. Beaurepaire, " Imaging lipid bodies in cells and tissues using third harmonic generation microscopy," Nature Methods **3**, 47-53 (2006).
10. A. M. Pena, T. Boulesteix, T. Dartigalongue, M. Strupler, E. Beaurepaire, and M. C. Schanne-Klein , "Chiroptical effects in the second harmonic generation from collagens I and IV: applications in nonlinear microscopy," Nonlinear Opt., Quantum Opt. **35** (2006).
11. S. Brasselet and J. Zyss, "Nonlinear polarimetry of molecular crystals down to the nanoscale," C. R. Physique **8**, 165-179 (2007).
12. C. Odin, Y. Le Grand, A. Renault, L. Gailhouste, and G. Baffet, "Orientation fields of nonlinear biological fibrils by second harmonic generation microscopy," J. Microsc. **229**, 32–38 (2008).
13. V. Le Floc'h, S. Brasselet, J. F. Roch, and J. Zyss, "Monitoring of orientation in molecular ensembles by polarization sensitive nonlinear microscopy," J. Phys. Chem. B **107**, 12403-12410 (2003).

#100156 - $15.00 USD Received 13 Aug 2008; revised 23 Sep 2008; accepted 24 Sep 2008; published 3 Dec 2008

14. C. Anceau, S. Brasselet, and J. Zyss, "Local orientational distribution of molecular monolayers probed by nonlinear microscopy," Chem. Phys. Lett. **411**, 98-102 (2005).
15. S. Brasselet, V. Le Floc'h, F. Treussart, J. F. Roch, J. Zyss, E. Botzung-Appert, and A. Ibanez, "In situ diagnostics of the crystalline nature of single organic nanocrystals by nonlinear microscopy," Phys. Rev. Lett. **92**, 207401 (2004).
16. D. Oron, D. Yelin, E. Tal, S. Raz, R. Fachima, and Y. Silberberg, "Depth-resolved structural imaging by third-harmonic generation microscopy," J. Struct. Biol. **147**, 3-11 (2004).
17. H. Wang, Y. Fu, P. Zickmund, R. Shi, and J.-X. Cheng, "Coherent Anti-Stokes Raman Scattering Imaging of Axonal Myelin in Live Spinal Tissues," Biophys. J.**89**, 581–591 (2005).
18. D. Lara and C. Dainty, "Axially resolved complete Mueller matrix confocal microscopy," Appl. Opt. **45**, 1917-1930 (2006).
19. C.E. Bigelow and T.H. Foster, "Confocal fluorescence polarization microscopy in turbid media: Effects of scattering-induced depolarisation," J. Opt. Soc. Am. A **23**, 2932 (2006).
20. T. brixner, G. krampert, P. niklaus, and G. gerber, "Generation and characterization of polarization-shaped femtosecond laser pulses," Appl. Phys. B **74**, S133–S144 (2002).
21. D. Oron, N. Dudovich, and Y. Silberberg, "Femtosecond Phase-and-Polarization Control for Background-Free Coherent Anti-Stokes Raman Spectroscopy," Phys. Rev. Lett. **90**, 213902 (2003).
22. Elijah Y. S. Yew, and Colin J. R. Sheppard, "Effects of axial field components on second harmonic generation microscopy," Opt. Express **14**, 1167-1174 (2006).
23. B. Richards and E. Wolf, "Electromagnetic diffraction in optical systems. II. Structure of the image field in an aplanetic system," Proc. R. Soc. London Ser. A. **153**, 358-579 (1959).
24. L. Novotny and B. Hecht, *Principles of Nano-Optics* (Cambridge University Press, Cambridge 2006).
25. D. Axelrod, "Carbocyanine dye orientation in red cell membrane studied by microscopic fluorescence polarization," Biophys. J. **26**, 557-574 (1979).
26. K. Komorowska, S. Brasselet, J. Zyss, L. Pourlsen, M. Jazdzyk, H. J. Egelhaaf, J. Gierschner, and M. Hanack, " Nanometric scale investigation of the nonlinear efficiency of perhydrotriphynylene inclusion compounds," Chem. Phys. **318**, 12-20 (2005).

1. Introduction

Manipulating optical polarization through a microscope objective in fluorescence and coherent nonlinear microscopy has raised a significant interest in imaging and spectroscopy. Polarization is widely used in anisotropy imaging in fluorescence at one and two photon excitation regimes, to investigate molecular order and organization in molecular and biomolecular media. Those studies are traditionally performed from the measurement of fluorescence anisotropy using a set of two states of incident polarization ("*s* and *p*" or "*V* and *H*") and two states of analyzed polarizations, resulting essentially in two accessible parameters $I_{//}$ and $I_{\perp}$ depending on the parallel or perpendicular configuration of the incident versus analyzed directions. However, this scheme has only been successful in cases limited to molecular angular distributions of cylindrical symmetry. It also contains redundancies such as the impossibility to differentiate the cases of an isotropic distribution from that of a 45° (relative to the *s* or *p* directions) molecular orientation. Fluorescence anisotropy imaging has nevertheless allowed functional contrasts in isotropic intracellular media [1,2], or for the determination of molecular angular distribution parameters such as the width of a cylindrical-symmetry distribution [3,4] or a mean molecular orientation angle [5,6]. Deciphering molecular and biomolecular behaviors however generally deals with complex molecular angular distributions that can strongly differ from purely cylindrical symmetry [7] and therefore require new and refined polarimetric analyses.

The development of multi-photon nonlinear microscopy involving a wide range of contrasts like fluorescence, second and third harmonic generation (SHG-THG), or Coherent Anti-Stokes Raman Scattering (CARS), have shown the possibility to reveal relevant biological contrasts with sub-micrometric intrinsic spatial resolution and sub-millimetric depth penetration, opening new routes towards the optical diagnostics of biological behaviors in complex cellular assemblies and tissues [8,9]. Attempts to complete these diagnostics with polarimetric analyses have raised in the study on chirality in biomolecular and molecular assemblies [10], and on molecular order from crystalline molecular systems to biological structures [12,13]. Recent works in polarized two-photon microscopy have demonstrated that rich information is contained in polarization responses recorded from an incident linear

#100156 - $15.00 USD Received 13 Aug 2008; revised 23 Sep 2008; accepted 24 Sep 2008; published 3 Dec 2008

polarization rotation, taking advantage of the nonlinear nature of the excitation which reduces the angular photoselection and thus ameliorates the angular sensitivity of polarized measurements [13,14]. Two-photon excitation fluorescence (TPEF) and SHG polarization resolved studies have been proposed to provide information on symmetry orders in complex orientational distributions in organized organic media : SHG being sensitive to asymmetry and odd orders in molecular angular distribution, a polarimetric SHG analysis is able to distinguish specifically and locally the nature (symmetry, disorder) of molecular assemblies in molecular monolayers [14] and in crystals down to the nanometric scale [15]. Polarization-controlled contrast improvement schemes have been also applied to THG [16] and CARS [17]. Such techniques are progressively applied to imaging in scattering media such as tissues, which will ultimately impose the use of techniques directly derived from ellipsometry such as the Mueller matrices formalism currently developed in scattered light analysis [18,19]. In this situation, polarization analysis can potentially improve image quality and resolution, allowing for instance the rejection of background from biomolecules' auto-fluorescence. At last, recently, polarization pulse shaping has appeared as a novel tool to exploit nonlinear light-matter interactions towards contrast enhancement [20,21]. This technique involves the spectral encoding, in a single ultrashort pulse, of many polarization states using spatial light modulators.

Whereas proofs of principle of polarization resolved nonlinear microscopy have clearly shown its potential, it requires the control of the excitation polarization state at the focal spot of an objective, which is a delicate task. An excitation polarization fixed at the entrance of a microscope, as required in inverted microscopy, will in particular be affected by reflection optics (principally the dichroic beamsplitter) and high numerical aperture focusing. The first effect has been identified for polarization-tuning two-photon inverted microscopy, where the determination of the dichroism factor and ellipticity induced by the dichroic beamsplitter was evidenced in the polarization response of a fluorescent isotropic sample made of molecules immobilized in a polymer layer [13]. Determining the polarization distortion parameters using this approach was however limited since it required the knowledge of the degree of homo-excitation energy transfer and the angle between the excitation and emission dipoles of the fluorophores, factors depending on the molecules and their concentration in the sample. The second effect occurs primarily when molecular excitation dipoles possess an orientation component along the normal direction of the sample, due to coupling with the axial component of the excitation field. This phenomenon has been mainly described in the context of coherent emission of second harmonic generation in objects of known symmetries [22].

In the present work, we investigate the effect of reflection optics and high numerical aperture focusing on two-photon fluorescence polarization responses in model samples. Polarization aberrations, appearing to a less extend, will not be considered in this work. We present a simple and robust technique to determine, in the sample plane, the degree of dichroism and ellipticity present in the (initially linear) excitation polarization at the focus spot of a nonlinear microscope. This method uses a reference liquid fluorescent sample from which the polarization read-out is independent on either the molecule or its concentration. We illustrate the use of this technique to determine dichroism and ellipticities (in the $[0\text{-}\pi/2]$ range), and propose a scheme to read-out ellipticities in the $[0\text{-}\pi]$ range without ambiguity. In addition to these experimental demonstrations, a numerical calculation of the emitted signal is performed in order to quantify the contribution of polarization spatial distortions induced by the high numerical aperture focusing.

2. Two-photon fluorescence polarization response in high numerical aperture focusing microscopy

In this section we analyze the features of two-photon fluorescence (TPF) polarimetry under a linearly tunable incident polarization at the entrance of the microscope, accounting for possible experimental factors inducing polarization distortions. The incident field in the sample plane is decomposed on the (x_1, x_2, x_3) macroscopic frame (Fig. 1).

#100156 - $15.00 USD Received 13 Aug 2008; revised 23 Sep 2008; accepted 24 Sep 2008; published 3 Dec 2008

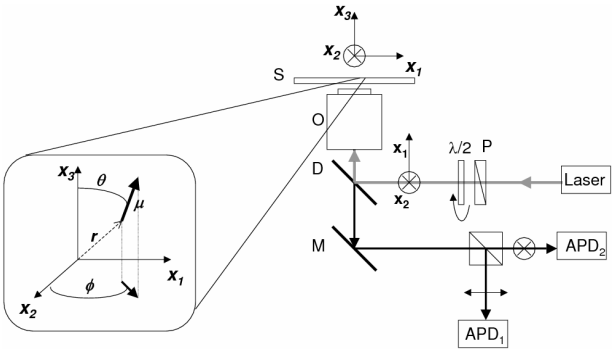

Fig. 1. Geometry of the polarimetric two-photon fluorescence microscopy, also corresponding to the set-up used : O : objective (NA 1.2, x 60, Water Immersion), D : Dichroic mirror, M : mirror, $APD_{1,2}$: avalanche photodiodes detecting respectively the x_1 and x_2 components of the signal. P : polarizer, λ/2 : rotatable half waveplate. $\boldsymbol{\mu}$: fluorescence excitation dipole vector at position $\mathbf{r}$ and orientation $\Omega = (\theta,\phi)$.

The fluorescence intensity analyzed along a given polarization direction i is proportional to the two-photon absorption probability multiplied by the probability of emission in that direction, which, in a molecular ensemble, can be written as:

$$I_i(\alpha) = \iiint \overline{\left|\boldsymbol{\mu}_{abs}(\Omega,\mathbf{r})\cdot \boldsymbol{E}(\alpha,\mathbf{r})\right|^4} \left|\boldsymbol{E}_{em}(\Omega,\mathbf{r},\mathbf{k})\cdot \mathbf{u}_i\right|^2 f(\Omega) d\Omega\, d\mathbf{r}\, d\mathbf{k} \qquad (1)$$

where $\overline{\ldots}$ represents the time average, $f(\Omega)$ denotes the normalized molecular orientation distribution function, and $i = (x_1,x_2)$ is the analysed direction for a field propagating in the x_3 direction (Fig. 1). The incident electric field $\boldsymbol{E}(\alpha,\mathbf{r})$ polarized in the direction α (with respect to the x_1 axis) interacts at location $\mathbf{r}$ with the absorption dipole $\boldsymbol{\mu}_{abs}(\Omega,\mathbf{r})$, whose orientation is given by the angle set $\Omega = (\theta,\phi)$ (Fig. 1). The far field $\boldsymbol{E}_{em}(\Omega,\mathbf{r},\mathbf{k})$ is radiated by the emission dipole $\boldsymbol{\mu}_{em}(\Omega,\mathbf{r})$, in the propagation direction $\mathbf{k}$, with $\boldsymbol{E}_{em}(\Omega,\mathbf{r},\mathbf{k}) \propto \mathbf{k}\times(\mathbf{k}\times\boldsymbol{\mu}_{em}(\Omega,\mathbf{r}))$. $\mathbf{u}_i$ is a normalized vector in the i analysis polarization direction. In a polarimetric measurement α can be considered as a tuning parameter, its continuous variation defining the polarization response from the sample. This approach provides information on the distribution function $f(\Omega)$, independently on its symmetry and orientation [11], contrary to traditional anisotropy measurements. The final integration over all the possible molecular orientations (Ω), dipole positions in the excitation volume ($\mathbf{r}$), and emission angles within the collection aperture ($\mathbf{k}$), originates from the incoherent nature of the fluorescence emission. Coherent nonlinear processes such as SHG can be derived from this approach, accounting for coherent summations of fields radiated from induced nonlinear dipoles [11,13].

We consider now the case of an isotropic liquid under a two-photon excitation, with $f(\Omega)$=1. As in this situation the rotation diffusion time scale is shorter than the molecules' typical fluorescence lifetimes, the orientation of the absorption dipole is decorrelated from that of the emission dipole and one can define $\boldsymbol{\mu}_{abs}(\Omega,\mathbf{r})$ and $\boldsymbol{\mu}_{em}(\Omega',\mathbf{r}')$ with two independent orientations Ω and Ω'. Eq. (1) can then be written as:

$$I_i(\alpha) = \iint \overline{\left|\boldsymbol{\mu}_{abs}(\Omega,\mathbf{r})\cdot E(\alpha,\mathbf{r})\right|^4} d\Omega'\, d\mathbf{r} \iiint \left|\boldsymbol{E}_{em}(\Omega',\mathbf{r}',\mathbf{k})\cdot \mathbf{u}_i\right|^2 d\Omega'\, d\mathbf{r}'\, d\mathbf{k} \qquad (2)$$

The emission probability is seen to not depend on the incident polarization and as a consequence contributes only as a multiplicative constant when this polarization is tuned.

#100156 - $15.00 USD Received 13 Aug 2008; revised 23 Sep 2008; accepted 24 Sep 2008; published 3 Dec 2008

Therefore the collection aperture has no effect on the polarimetric response of the emitted signal and will only affect its global efficiency. The study of the polarization response of the fluorescence emission depends thus only on the absorption probability:

$$I_i(\alpha) = C_i \iint \overline{\left|\boldsymbol{\mu}_{abs}(\Omega, \boldsymbol{r}) \cdot \boldsymbol{E}(\alpha, \boldsymbol{r})\right|^4} d\Omega' d\boldsymbol{r} \tag{3}$$

where the *i*-dependent factor C_i, containing the emitted field radiation factor, may differ from different collection efficiencies along x_1 and x_2.

This expression shows in addition that contrary to isotropic materials made of fixed molecules such as in a polymer matrix [13], the emission and excitation dependencies can be decoupled, which ensures that the result is not affected by correlation-related issues such as fluorescence energy transfer or angles between the absorption and emission dipoles in the used molecules. The result is therefore independent on the molecules and their concentration.

Now introducing the incident field as originating from a rotated linear polarization possibly affected by a degree of ellipticity and of dichroism, the incident field amplitude at the entrance of the objective can be written:

$$\boldsymbol{E}(\alpha, \delta, \gamma) = \frac{E}{\sqrt{1 + (1-\gamma)^2}} \begin{bmatrix} \cos\alpha \\ (1-\gamma)\sin\alpha\, e^{i\delta} \\ 0 \end{bmatrix} \tag{4}$$

with δ being the phase difference (ellipiticity) and γ the amplitude factor (dichroism) between the two perpendicular polarization states *s* and *p* (defined by $\alpha = 0$, $\alpha = \pi/2$ or by the x_1 and x_2 directions in the sample plane). By nature these polarization directions are kept linear whatever the dichroic parameters, therefore only the intermediate polarizations are affected by the ellipticity.

We consider finally the focusing of the incident beam and the high numerical aperture collection. When focussed, a small component in the field's direction of propagation appears, increasing with the numerical aperture. The incident beam polarization state will depend on the space coordinates in the excitation volume and is now written $\boldsymbol{E}(\alpha, \delta, \gamma, \boldsymbol{r})$, with an expression previously published [22-24]. To take this spatial dependence into account the excitation volume is filled by a set of 300 regularly spaced dipoles, at whose locations the vectorial excitation field is estimated and used in Eq. (1). The collection aperture is then accounted for by expressing the radiated fields for all collected angles after the passage of the objective, following a procedure described previously [13,25]. The intensities of all dipoles are then summed up due to the incoherent character of the fluorescence emission. In a solution where the excitation process is randomized, the fluorescence polarimetric response is seen to be independent on the objective's numerical aperture both in the excitation and collection modes. Besides, as the fluorescence emission does not depend on the analysis direction, both intensities Ix_1 and Ix_2 are conserved. This situation is therefore adequate to study the polarization state distortions brought by the reflection optics. In the case of an anisotropic sample presenting out-of plane orientation directions, a coupling in the x_3 direction is possible and will affect the polarization response of the sample.

2.1 Polarization distortion by reflection optics

The previous analysis shows that a fluorescent solution is adequate to sort out information on polarization distortion by reflection optics. Figures 2(a) and 2(b) show the effect of the ellipticity δ and the amplitude factor γ on polar diagrams representing the fluorescence intensity as function of the incident polarization α in a fluorescent solution. When no ellipticity and dichroism factors are present, the response is angle-independent, as expected

#100156 - $15.00 USD Received 13 Aug 2008; revised 23 Sep 2008; accepted 24 Sep 2008; published 3 Dec 2008

from an isotropic solution. The ellipticity δ reduces the excitation efficiency at intermediate polarizations, the minimum efficiency occurring when the incident polarization is equal to π/4 modulo π/2. Contrary to δ, the γ factor is seen to affect the intensities in the x_1 and x_2 polarization directions: when its value is negative (resp. positive) the fluorescence is indeed the most efficient for an incident polarization parallel to the x_2 (resp. x_1) axis. Note that the effect of the δ factor on the fluorescence polarization response is only visible in the [0-π/2] range, due to the fact that in the isotropic summation of Eq. (3) the overall detected response is sensitive to a $|\cos 2\delta|$ dependence. Only polarization responses from non-isotropic molecular angular distributions will be able to raise the uncertainty of the [0-π/2] versus [π/2-π] range for δ. This is illustrated in Fig. 2c where a fixed 1D fluorescent sample (such as a crystal) has been modelled with an intermediate in-plane orientation of 2π/9. In this case Eq. (1) was derived with $f(\Omega) = \delta(\Omega - \Omega_0)$, taking a collection of dipoles in the excitation volume fixed in the direction $\Omega_0 = (\theta_0, \phi_0) = (\pi/2, 2\pi/9)$. In this situation the TPF polarization response is seen to be strongly dependent on the polarization parameters of the dichroic used.

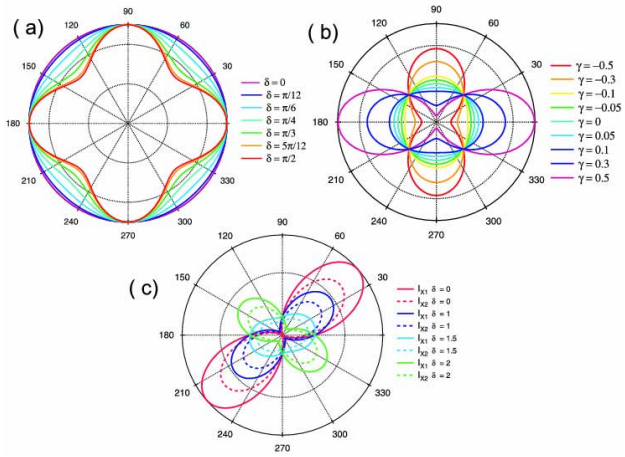

Fig. 2. Effect of the dichroic mirror parameters γ and δ (δ in rad) on the TPF polarization response represented as a polar graph in a solution (a,b) and a 1D fluorescent sample oriented at (θ, ϕ)=(π/2 , 2π/9) in the sample plane (c) (see Fig. 1 for angle definitions). (a,c) : influence of the ellipticity δ for an amplitude factor γ=0. (b) : influence of γ for δ=0. Continuous lines : Ix_1, dashed lines : Ix_2. The polarization responses are normalized to a maximum value of 1.

When δ=0, the polarization response is anisotropic in the 2π/9 (40°) direction as expected from the 1D symmetry of the sample. As the ellipticity increases, the polarization response changes its direction, until reaching another quadrant for δ>π/2. This example emphasizes the detrimental influence of in-plane polarization ellipticity when performing polarimetric measurements, the response being indeed strongly distorted for high ellipticities. As expected, this geometry allows a discrimination of the range of the ellipticity : a polarization response stays in the quadrant of the sample orientation for to 0<δ<π/2, whereas the response reaches the next quadrant for π/2<δ<π, due to polarization rotation.

It appears finally from this model that the continuous rotation of a polarization allows extraction of the polarization perturbations induced by the dichroic beamsplitter with an ellipticity wrapped in the [0-π/2] range, independently on the high numerical aperture focusing and collection. The ellipticity range indetermination can be eventually raised with an anisotropic sample. The (γ,δ) determination in fact requires only three measurements $I_i(0)$, $I_i(\pi/4)$ and $I_i(\pi/2)$. The solution is also unique as described in Fig. 3 representing the

#100156 - $15.00 USD Received 13 Aug 2008; revised 23 Sep 2008; accepted 24 Sep 2008; published 3 Dec 2008

cartographies of the ratios $I_i(\pi/2)/I_i(0)$ and $I_i(\pi/4)/I_i(0)$ in a (γ,δ) coordinates map. A given value of the ratio $I_i(\pi/2)/I_i(0)$ corresponds to a vertical line in the (γ,δ)-map (Fig. 3(a)), this ratio being independent on the ellipticity of the dichroic beamsplitter, whereas a given value of the ratio $I_i(\pi/4)/I_i(0)$ corresponds to a curve that is (γ,δ)-dependent (Fig. 3(b)). The interception between both curves is therefore a single point in the (γ,δ)-diagram. Taking into account typical experimental uncertainties (see below), the solution space for each ratio will no longer be a single line but a band with certain error-width, as shown in Fig. 3(c). For a better experimental estimation a fit of the polarization dependent TPF-signal should be considered, as described in the next section.

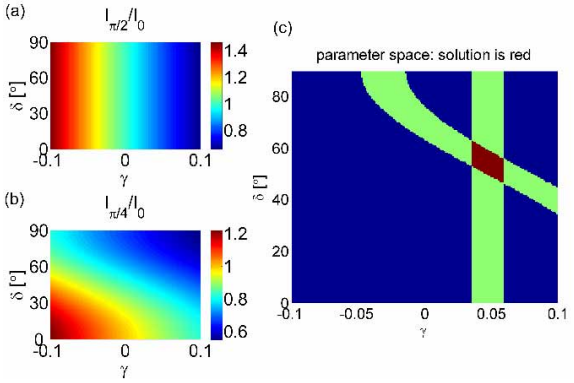

Fig. 3. Cartographic map of the fluorescence intensity ratios (a) $I_i(\pi/2)/I_i(0)$ and (b) $I_i(\pi/4)/I_i(0)$ as functions of the dichroic parameters (γ,δ) (δ in °). (c) : Typical solution (red space) including experimental error margins for a three-point-fit.

2.2 Polarization distortion by high NA focussing

As detailed above, a fluorescence polarization response measurement of a solution is independent on high NA focusing. This is however not the case in typical measurements which involve samples with complex symmetries. To illustrate the role of the high NA used in two-photon microscopy, a model system of 1D symmetry was used in the calculation of Eq. (1) accounting for the whole vectorial form of the spatial excitation field. Fig. 4 depicts the polarization TPF response of a 1D sample made of fixed dipoles orientation, with small ($\theta = \pi/3$) and strong ($\theta = \pi/6$) orientation components along x_3. At low numerical aperture (NA = 0.1) the polarization response is only slightly deformed by an off-plane tilt. In the high numerical aperture (NA = 1.2) case however, strong deformations in the polarization response appear. The apparition of a background signal leads in particular to a response that can be mislead with that from a non-1D sample. Note that while the observed deformation exists even for $\delta, \gamma = 0$, it is enhanced with increasing ellipticities δ. In practice it is therefore crucial to account for the high NA focussing in order to model the whole 3D picture of the distribution function of fluorescent molecules. Note also that the high NA collection would lead only to a modification of the Ix_1/Ix_2 overall ratio but not to a deformation of the polarization response. Measuring separately these two components can be particularly advantageous to discriminate ordered verses disordered molecular assemblies [11].

#100156 - $15.00 USD Received 13 Aug 2008; revised 23 Sep 2008; accepted 24 Sep 2008; published 3 Dec 2008

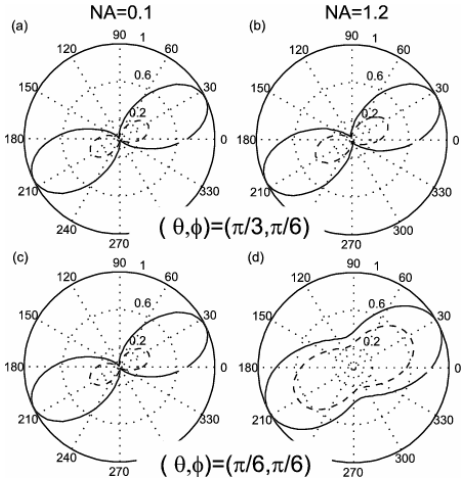

Fig. 4. TPF polarization responses of a 1D fluorescence sample accounting for both reflection optics (using the parameters $\delta = \pi/4$, $\gamma = 0.01$) and high numerical aperture focussing (a,c) : NA = 0.1, (b,d) : NA = 1.2 . Sample orientation (see Fig. 1 for angle definitions) (a,b) : $(\theta, \phi)=(\pi/3, \pi/6)$, (c,d) : $(\theta, \phi)=(\pi/6, \pi/6)$. Continuous line : Ix_1, dashed line : Ix_2. The polarization responses are normalized to a maximum value of 1.

3. Experimental calibration

The retrieval of the polarization parameters introduced by reflection optics has been investigated experimentally using a typical two-photon microscopy inverted set-up represented in Fig. 1. A mode-locked Ti:Sa laser (Chameleon by Coherent, Santa Clara, CA) is used as the excitation source producing 150 fs pulses with a repetition rate of 80 MHz, whose center wavelength can be tuned between 680 nm and 1050 nm. After the passage of a horizontal polarizer the input field's polarization can be rotated by an achromatic half waveplate mounted in a step rotation motor. The incident field is reflected by a dichroic beamsplitter (650DCXP Chroma, Rockingham, VT) before being focused by a high numerical aperture (x60, NA = 1.2) water immersion objective (Nikon) into a solution of free Rhodamine 6G diluted in water (at about 10^{-4} mol/l concentration). The generated TPF signal is collected by the same objective, traverses the dichroic beamsplitter and is finally divided by a polarization beam splitter according to its principal polarization axes and sent to two avalanche photodiodes. As mentioned in the previous section, the determination of the dichroic parameters γ and δ gained in precision by fitting the whole polarization dependent TPF signal. For this, theoretical curves were calculated for a large variety of (γ,δ)-values and compared with our experimental data, the sum of mean squares (χ^2) being an indication of the concordance. Figure 5 shows the dependence of χ^2 on δ and γ for a measurement at λ = 900 nm. Only one minimum exists, which allows a subsequent fitting procedure starting at any point in the (γ,δ)-space to find the global minimum by minimizing alternately both parameters until a stable χ^2 is reached. Note that a slight asymmetry is observed in the experimental polarization response, which is assigned to a surface heterogeneity in the optics used. The consequence is a slight increase in the ellipticity error margin, which was still estimated at less than 10^{-2} rad.

#100156 - $15.00 USD Received 13 Aug 2008; revised 23 Sep 2008; accepted 24 Sep 2008; published 3 Dec 2008

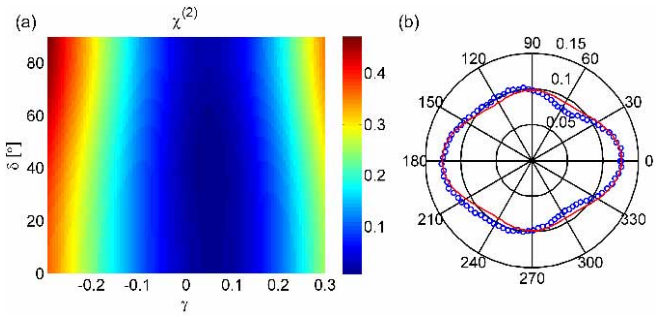

Fig. 5. Experimental measurement of a polarimetric response from a Rh6G solution excited at 900nm : (a) χ^2 parameter represented for a range of (δ, γ) (δ in °), (b) : experimental points (dots) and corresponding fit (continuous line).

The results of this approach for a large variety of wavelengths are shown in Fig. 6 together with some examples of the corresponding TPF signals. As stated above, the determination of the δ factor is made within a [0-π/2] range.

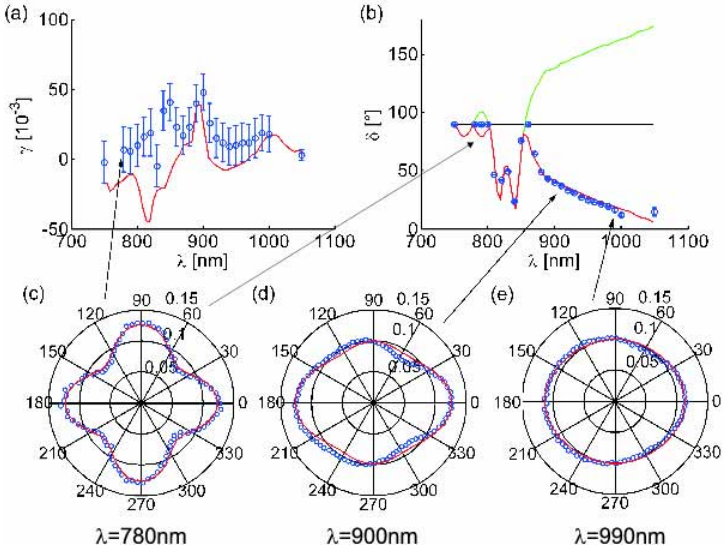

Fig. 6. δ (a) and γ (b) parameters deduced from the TPF polarization responses (dots) and ellipsometry data (continuous line) on the dichroic mirror used for two-photon fluorescence, at various incident wavelengths. Each experimental point results from a 6 measurements. The green line in (b) corresponds to the δ ellipsometry data while the red one is wrapped in the [0-π/2] range for comparison with polarimetric measurements. (c-e) TPF polarization responses and fits (red curves) at three different wavelengths : (c) : 780nm, (d) :900nm, (e) : 990nm.

In order to confirm the origin of the retrieved parameters, we measured the expected δ and γ values from the dichroic mirror at 45° incidence by ellipsometry (GESP5 Sopra). The measured *p/s* reflection polarization ratio $r_p / r_s = (1-\gamma).e^{i\delta}$ gives a direct access to the unknown γ and δ values, without phase ambiguity. As can be seen in Fig. 6, the measured parameters in the two-photon fluorescence microscope are in good agreement with the ellipsometry measurement for the whole wavelength range explored. The comparison of the data necessitated a phase wrapping of the ellipsometric date in the [0-π/2] range. This good agreement confirms that δ and γ are almost exclusively caused by the dichroic itself and not by other optical components. Note that while the dichroic factor γ is seen to lie close to 0

#100156 - $15.00 USD Received 13 Aug 2008; revised 23 Sep 2008; accepted 24 Sep 2008; published 3 Dec 2008

(which ensures a small deviation of the amplitude *p*/*s* ratio from 1), the ellipticity caused by the dichroic mirror can reach high values far above π/2. This causes an intermediate incoming polarization to become elliptic and potentially rotated, which strongly affects polarization responses (Fig. 2(c)). Other two-photon excitation dichroic mirrors studied with the same technique showed similar behaviours, especially close to their cut-off wavelength.

To illustrate the dramatic changes brought by polarization in-plane ellipticity on experimental polarization responses in anisotropic samples, measurements were performed in a 1D fluorescent sample made of oriented fluorescent molecules along a macroscopic crystal axis, which macroscopic orientation can be identified visually. This sample is a Perhydrotriphenylene (PHTP)-4-Dimethylamino-40-nitrostilbene (DANS) co-crystal characterized in a previous work [26], oriented at an angle close to 30° in the plane of the sample (Fig. 7). The polarization responses are fitted using the previously determined parameters δ and γ. The 1D crystalline model fitting leads to $\Omega_0 = (\theta_0, \phi_0) = (90°, 29°)$, which is close in agreement with the initially set crystal orientation as seen in its fluorescence image (Fig. 7(a)). The fit is therefore shown to be in excellent agreement with the expected values for the dichroic parameters. In the 975nm case, the value $\delta > \pi/2$ causes the orientation of the polarimetric response to be un-correlated with the initial crystal orientation. This examples shows in addition that no off-plane component exists in the present molecular orientation, since the high NA focusing in this case does not affect the quality of the fit.

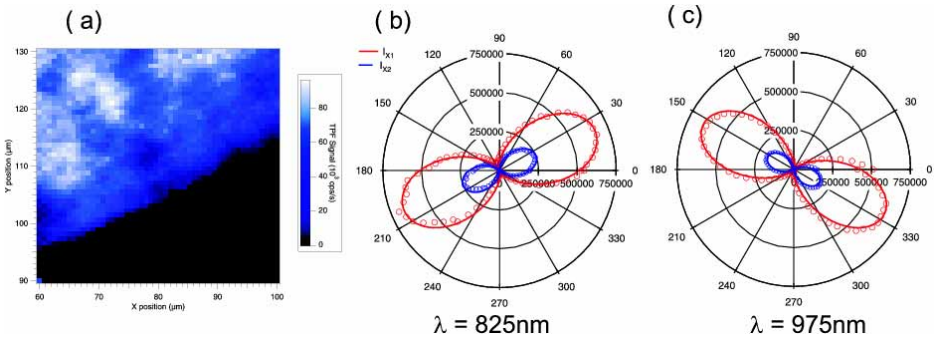

Fig. 7. TPF polarization response of a 1D crystalline fluorescence sample made of DANS molecules in a PHTP crystalline host : (a) 2D scan (by a piezoelectric stage) of the sample showing the macroscopic crystal orientation, (b,c) : experimental data (dots), and corresponding fits (continuous line) at (b) 825nm excitation and (c) 975nm excitation wavelengths. The fits account for the measured dichroic parameters and for the molecular orientation (θ_0, ϕ_0)=(90°, 29°).

4. Summary

We have shown the effect of experimental parameters in TPF polarization response investigations, in particular polarization distortions due to a dichroic beamsplitter reflection and high NA focusing effects in a 3D sample geometry. This study can be extended to other nonlinear contrasts including coherent optical effects. We demonstrated that using a simple polarization rotation scheme in a solution, the polarization ellipsometric parameters of the incident excitation in the sample plane could be determined. Ellipticities are determined in a [0-π/2] range, the phase uncertainty being raised from an observation in anisotropic samples. Once such parameters are determined, the orientational information from a local point of the sample of interest can be determined without ambiguity, as exemplified in a crystalline sample (Fig. 7). This study can be extended to the determination of more complex angular distributions, implementing for instance in Eq. (1) a Legendre polynomial decomposition of the unknown distribution function [11,14]. This scheme, thanks to its simplicity, can be useful

#100156 - $15.00 USD Received 13 Aug 2008; revised 23 Sep 2008; accepted 24 Sep 2008; published 3 Dec 2008

for calibration of experiments where complex polarization excitation states need to be engineered in the sample plane, such as for Mueller matrices exploration or polarization pulse shaping applications.

Acknowledgments

The authors would like to thank Chi Thanh Nguyen (ENS Cachan, Laboratoire de Photonique Quantique et Moléculaire) for his precious help on the ellipsometric characterization of the dichroic beamsplitters. This work is supported by the French ministry of Research, through the ANR Jeunes Chercheurs “NLO Shaping” contract ANR_JC07_195504.

#100156 - $15.00 USD Received 13 Aug 2008; revised 23 Sep 2008; accepted 24 Sep 2008; published 3 Dec 2008